

## Formation of Filamentous Carbon from Iron, Cobalt and Chromium Catalyzed Decomposition of Acetylene

R. T. K. BAKER, P. S. HARRIS, R. B. THOMAS, AND R. J. WAITE

*Applied Chemistry Division, Building 10.5, Atomic Energy Research Establishment, Harwell, Didcot, Berkshire, U. K.*

Received October 20, 1972

The formation of filamentous carbon from iron, cobalt and chromium catalyzed decomposition of acetylene has been studied by controlled atmosphere electron microscopy. The behavior of these metals when supported on graphite and silicon has been investigated. Detailed analysis of filament growth sequences gave activation energies for filament growth which show excellent agreement with those for diffusion of carbon through the corresponding metals. An inverse dependence of catalyst particle size with growth rate was found, the coefficient of which is also inversely proportional to temperature. These observations are consistent with, and provide further support for, the proposed mechanism for filament growth.

### INTRODUCTION

Interest in catalytic decomposition of hydrocarbons on metallic surfaces has recently become more active (1-6). Palmer and Cullis (7) have reviewed work up to 1965. The most active catalysts for carbon formation are the transition metals iron, cobalt and nickel, but the precise mechanism and nature of the catalyst in many of these systems is still not definitely established.

As shown in a previous paper (1), at least three types of carbon are produced from the nickel catalyzed decomposition of acetylene. Mechanisms were suggested for the role of nickel in the formation of flocculent, filamentous and platelet deposits. In the present work we have examined the catalytic effects of iron, cobalt and chromium in the presence of acetylene and compared the characteristics of the filamentous carbon produced in these systems with that produced in the presence of nickel catalysts.

### METHODS

#### *Technique*

The technique of controlled atmosphere electron microscopy has been described in

detail elsewhere (8). Incorporation of a gas reaction cell within a JEM 7A electron microscope allows for continuous observation of dynamic reactions occurring between gases and solids to be made at high magnifications. The transmission image is displayed on a television monitor and continuously recorded on video tape. Detailed quantitative analysis is achieved by single frame projection of a 16 mm cine film of the video record.

#### *Materials*

The single crystal graphite supports used in these experiments were prepared from crystals obtained from Ticonderoga, New York State, by a standard method (1). Silicon support films were prepared by evaporation of silicon crystals (Sherman Chemicals Ltd. 99.95% purity) in a similar manner to that described for the preparation of silica films (1). Iron and cobalt were deposited onto the support materials as thin films by evaporation of the respective spectrographically pure metal wires at a residual pressure of  $10.0 \text{ mN m}^{-2}$  from a heated tungsten filament. Chromium was transferred to the support media by one of two methods: (a) rapid evaporation from

a tungsten boat at 10.0 mN m<sup>-2</sup> or (b) as a drop of a suspension of Cr<sub>2</sub>O<sub>3</sub> in isopropanol. This was prepared by decomposition of ammonium dichromate followed by calcining in air at red heat for 5 hr. The specimen was heated in hydrogen at 1075 K for 30 min before reaction with acetylene.

The reactant gases used in these experiments, acetylene, hydrogen (Air Products Ltd.) and oxygen (British Oxygen Co. Ltd.) all >99% purity, were used without further purification.

### RESULTS

On heating, the metal films were observed to nucleate into small particles (~10 nm diam) as specimen temperatures reached 775 K in 0.3 kN m<sup>-2</sup> acetylene. As the temperature was raised further, several forms of carbonaceous deposit were formed including amorphous, filamentous and graphitic. In this study attention was focused solely on the formation of filamentous carbon, and the main events of interest which occurred in the different systems are reported in the following sections.

#### Common Characteristics of the Systems

Conditions under which filament growth was studied are shown in Table 1. The common characteristics were:

a. All filaments had a particle at their growing end as was observed with those produced from Ni/C<sub>2</sub>H<sub>2</sub> (1).

b. The diameter of the filaments was controlled by that of the catalyst particle, the latter being fractionally the smaller in most cases. Filament diameters varied from

10 to 150 nm and the lengths from 0.5 to 8.0 μm, over the range 785 to 1245 K.

c. The filaments grew with random paths forming loops, spirals, and interconnected networks. Graphs showing the relation of filament length to time for Fe/C<sub>2</sub>H<sub>2</sub> and Co/C<sub>2</sub>H<sub>2</sub> systems were similar in shape to those found for the Ni/C<sub>2</sub>H<sub>2</sub> system (1), and a definite constant growth rate region (zone 2) was observed [Fig. 1 (cf. Ni/C<sub>2</sub>H<sub>2</sub>)]. Growth times to termination were dependent on temperature: At 925 K some filament growth sequences were followed for 10 min, whereas at 1245 K growth ceased after 30 sec.

d. High magnification examination of a filament which had ceased to grow, showed that the catalyst particle at the growing end was completely enveloped by a layer of deposit. Similar examination of a filament whose growth had been deliberately arrested by a rapid decrease of the temperature showed that the front face of the catalyst particle had no layer of deposit.

e. Postreaction examination revealed many of the structural features of the filaments. Figure 2 is a detailed micrograph of a typical filament showing the "pear-shaped" catalyst particle at the head of the filament. It is possible to trace the path of an electron transparent channel, which permeates the length of the filament, to the apex of the catalyst particle.

f. When the filaments from Fe/C<sub>2</sub>H<sub>2</sub> and Co/C<sub>2</sub>H<sub>2</sub> systems were exposed to 1.3 kN m<sup>-2</sup> oxygen they reacted in a similar manner to those produced from Ni/C<sub>2</sub>H<sub>2</sub> (1). At 970 K the inner portion surrounding the

TABLE 1  
COMPARISON OF MEASURED ACTIVATION ENERGIES FOR FILAMENT GROWTH WITH THOSE FOR CARBON DIFFUSION IN THE CORRESPONDING METAL CATALYSTS

Metal	Activation energy for		Temp range studied (K)	Pressures (kN m <sup>-2</sup> )
	Diffusion of carbon (kJ mol <sup>-1</sup> )	Catalyzed filamentous carbon growth		
α-Iron	43.9-69.0 (9)	67.3 ± 5	925-1245	0.3
Cobalt	144.9 (10)	138.1-139.2 ± 7.0	800-1200	0.07
Chromium	110.8 (11)	113.4 ± 15 <sup>a</sup>	785-1270	0.13
Nickel	138-145.5 (12)	145.0 (1)	—	—

<sup>a</sup> Estimated from only two points.

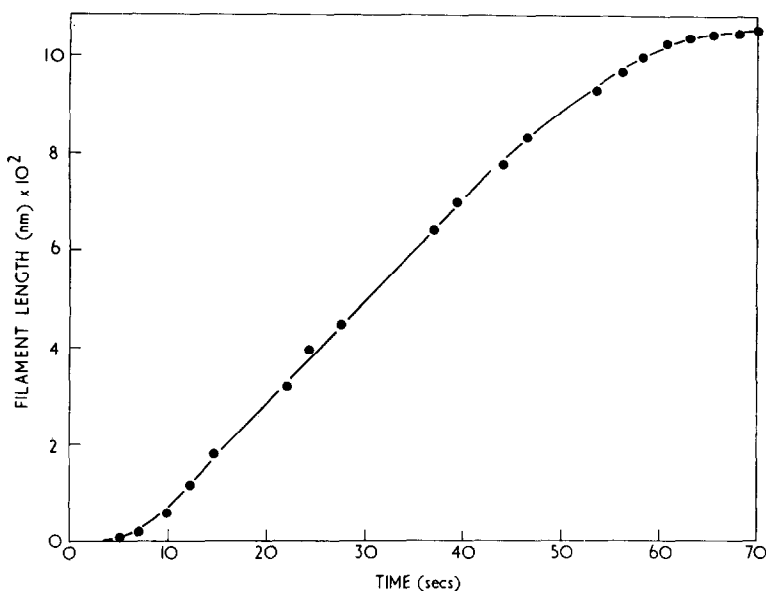


FIG. 1. Growth rate curve for filamentous carbon from iron catalyzed decomposition of  $0.3 \text{ kN m}^{-2}$  acetylene at 1010 K.

central hollow channel of the filaments had a reactivity towards oxygen similar to that of the amorphous carbon deposit, and oxidized first to reveal the presence of a relatively oxidation resistant filament wall material. These experiments suggest that filaments produced from all these metals have a similar structure, and from measurements of the larger diameter filaments the typical dimensions were:

Filament outer diam	150–130 nm
Diam of central core	95–85 nm (including a central hollow channel of 10 nm)
Thickness of filament wall	25–22 nm

If oxidation was continued, then at 1150 K the material constituting the wall of the filaments oxidized.

g. No evidence was found to indicate that particles as such could become embedded within the filament. Electron dense regions appeared along the filament, but by continuous observation it was possible to identify these zones as crossover sections. The possibility, however, that a thin layer of catalyst of atomic dimensions was left

behind on surfaces could not always be excluded.

h. There was a definite regular increase in filament growth rate with decreasing particle size; this relationship was determined quantitatively for iron (Fig. 3).

i. From plots of log rate against  $1/T$  activation energies for filamentary growth were estimated (Table 1). The activation energy was independent of particle size as shown in Fig. 4.

j. When excessive amounts of amorphous carbon were allowed to form before raising the temperature, filament formation was completely suppressed.

#### *Anomalous Behavior*

Active iron particles could undergo fragmentation, without loss of activity at temperatures above 1010 K, when supported on silicon. This phenomenon, which appeared to have an induction period of about 2 min can be seen in Fig. 5, from an experiment conducted at 1010 K and in the presence of  $0.3 \text{ kN m}^{-2}$  acetylene. Frames A and B show the growth of a filament from an iron particle, A (95 nm diam), and in frame C it is apparent that fragmentation of particle A



FIG. 2. Micrograph of a filament showing "pear-shaped" catalyst particle at its head.  $\times 120,000$ .

has occurred. In frame D, the growth of filaments from the fragmentary particles (50–20 nm diam) can be seen. Branching only occurred from the parent particle; secondary fragmentation of the smaller particles was not observed. From frame by frame analysis, a growth rate plot of this sequence gave a value of  $22.3 \text{ nm s}^{-1}$  for the filament growth rate from particle A

(95 nm diam) and after fragmentation two of the particles B (50 nm diam) and C (20 nm diam) gave filament growth rates of  $41.8$  and  $56.5 \text{ nm s}^{-1}$ , respectively. (Fragmentation and secondary filament growth only occurred when the iron particles were originally supported on silicon.)

The behavior of cobalt appeared to be quite independent of the nature of the sup-

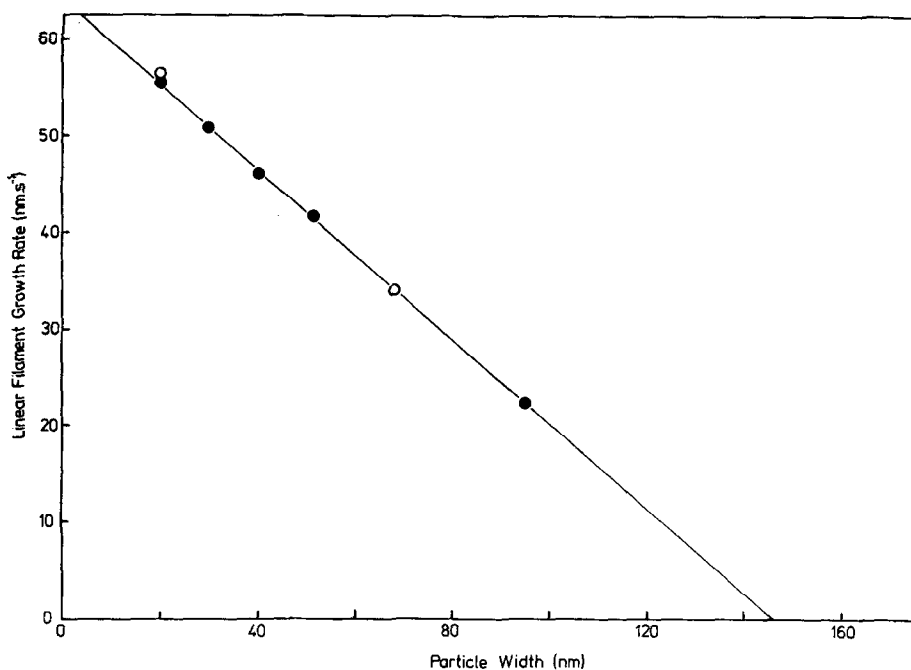


Fig. 3. Variation of the rate of filament elongation with catalyst diameter at 1010 K: (●) from primary particles; (○) from fragmentary particles.

port at temperatures up to 1075 K. Above this temperature, if a silicon support was used, finer secondary filaments ( $\sim 10$  nm diam) were propelled out of the leading face of the larger active cobalt particles ( $\sim 140$  nm diam). These secondary fila-

ments grew at a much faster linear rate and in the opposite direction to that of the main filaments, which maintained an uninterrupted growth rate. This effect can be seen in the sequence in Fig. 6, and was representative of the behavior of all the larger

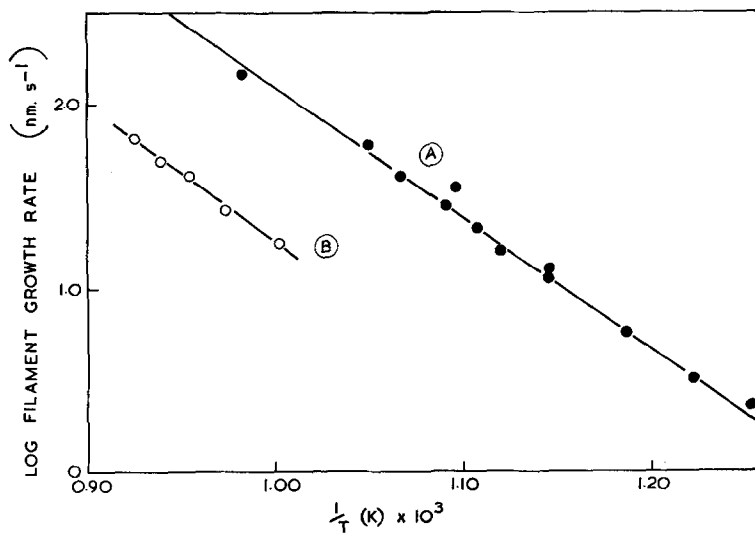


Fig. 4. Arrhenius plot for filamentous carbon growth from cobalt catalyzed decomposition of  $0.07 \text{ kN m}^{-2}$  acetylene: (A) for 20-40 nm diam particles; (B) for 120-140 nm diam particles.

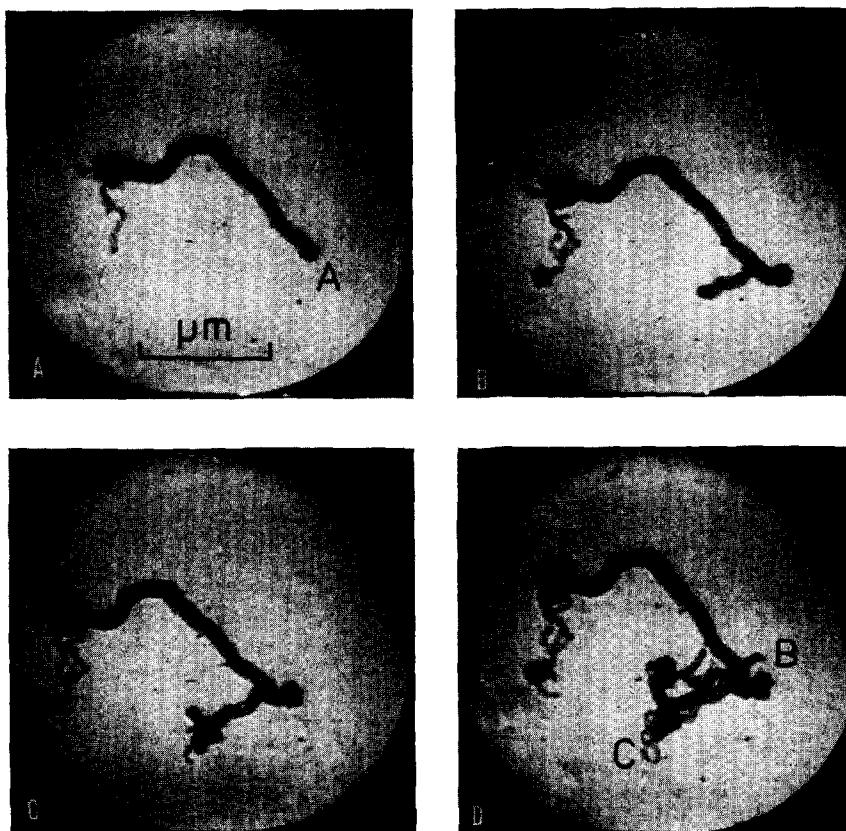


FIG. 5. Filament growth sequence from iron catalyzed decomposition of  $0.3 \text{ kN m}^{-2}$  acetylene at 1010 K on silicon support; time interval between frames is 20 sec. A = initial iron particle, B and C are fragmentary particles.  $\times 21,100$ .

particles above 1075 K. Secondary filament growth was not observed with cobalt particles supported on graphite in acetylene even at temperatures up to 1200 K. An indication that this phenomenon might be attributable to diffusion of silicon into the cobalt at elevated temperatures when the two are in physical contact was indicated from the following experiment. If small amounts of silicon impurities were introduced onto a previously nucleated cobalt/graphite specimen and were subsequently exposed to acetylene at temperatures above 1075 K, then secondary filament growths were observed on some of the metal particles.

The behavior of the chromium particles when supported on silicon and heated in the presence of  $0.13 \text{ kN m}^{-2}$  acetylene was quite different. In this system filamentous

carbon growth did not occur until 1075 K and an entirely new mode of filament growth was observed in which the carbon filament was extruded from the metal particle, which remained in contact with the silicon surface. The diameter of the active metal particle was in general larger than that of the growing filament and in some cases was a source of multiple filament formation.

#### DISCUSSION

The formation of the flocculent amorphous deposit has been discussed previously (1). It is probably derived from gas phase polymerization of acetylene and the role of the metal particles was simply that of nucleating centers for its accumulation on the surface.

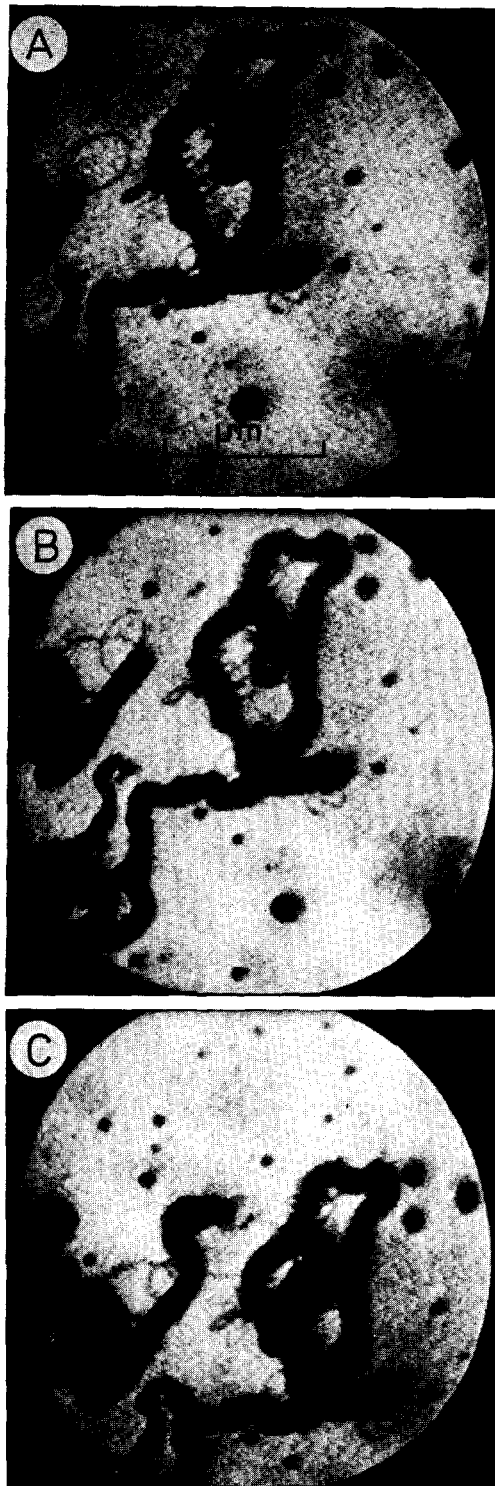


FIG. 6. Secondary filament growth from decomposition of  $0.07 \text{ kN m}^{-2}$  acetylene by cobalt supported on silicon, at  $1080 \text{ K}$ ; time intervals between frames A and B is 10 sec and frames B and C is 20 sec.  $\times 24,600$ .

### *Filamentous Growth*

A mechanism for the formation of filamentous carbon from nickel catalyzed decomposition of acetylene has been postulated (1), which depends on diffusion of carbon through the metal particle from the hotter leading face on which acetylene decomposition occurs to the cooler trailing faces at which carbon is deposited from solution. Growth ceases when the leading face is covered with carbon built up as a consequence of overall rate control by the carbon diffusion process.

With the exception of the Cr/C<sub>2</sub>H<sub>2</sub> system on a Si support, the filaments formed in the present experiments had all the structural characteristics of those grown from Ni/C<sub>2</sub>H<sub>2</sub> (1), and the observation that complete encapsulation of the catalyst particle was accompanied by a loss in activity indicates that filaments were produced in all these systems by a similar mechanism.

The activation energies for filament growth are compared with those for diffusion of carbon through the corresponding metals in Table 1. The excellent agreement between these two sets of data supports the assumption that diffusion of carbon through the metal is the rate determining step in the filament growth process, and indicates that this mechanism is operative with all these metals.

The inverse dependence of growth rate with particle width (Fig. 3) is also consistent with a diffusion controlled mechanism (Appendix). Moreover, the agreement between measured activation energies from small and large particles of cobalt shows that the rate dependence on particle size has a coefficient which is also inversely proportional to temperature. This dependence can be best understood by considering the mathematical approximation presented in Appendix. For reasons of simplicity the shape of the metal catalyst particle is treated as a cylindrical pellet or as a truncated cone. Solutions of the diffusion equation for both situations indicate that the linear filament growth rate varies inversely with the mean radius of the particle.

Although the proposed mechanism for

filamentous growth accounts for filaments produced from all these metals, there are major differences in their behavior when the metals were supported on silicon. These abnormal growth sequences all appear to take place in the same temperature region, and it seems reasonable to assume that silicon is, to some extent, incorporated into the metal particles at temperatures above 1000 K. Indeed, results from this laboratory (13) have shown that iron particles are capable of transporting significant amounts of silicon from a silicon support at these temperatures, when the two are in contact.

It was observed that active iron particles were subject to fragmentation at temperatures above 1010 K when supported on silicon and that the smaller particles produced were still active towards further filamentous growth. Moreover, the rate of filament growth from these particles showed the same dependence on size as those derived from primary particles (Fig. 3). This implies that whatever effect caused fragmentation it does not significantly alter the diffusion characteristics of carbon through iron. This branching phenomenon appeared to be quite characteristic of iron, and the delayed onset of fragmentation indicates that it is preceded by another slower process.

Baraniecki, Pinchbeck and Pickering (14) have shown that the presence of silicon will promote the formation of graphite from carbon dissolved in iron. Furthermore, they found that as the reaction proceeded the metal particles became increasingly disseminated. In a previous publication Baker, Feates and Harris (2) reported that graphite platelets were produced at the edges of iron particles saturated with carbon at 1175 K. If silicon impurities are promoting the precipitation of graphite from the iron particles in the present system, then the graphite would be expected to collect at the cooler regions of the particle, i.e., at the interface between the metal and the filament. This reaction would be relatively slow and eventually result in the deformation of the shape of the metal/filament interface. In this event the particle could rupture with the subsequent forma-



tion of branch filaments. Wagner and Doherty (15) have shown that branching in analogous vapor-liquid-solid systems is attributable to changes in the morphology of the liquid/solid interface.

With a silicon support, at temperatures of 1075 K and above, all filaments from chromium and secondary filaments from cobalt appear to grow by a similar extrusion mode. This type of growth has been observed in this laboratory when acetylene is decomposed over other alloy catalysts (16). Preliminary results indicate that the rate determining step in this new mechanism is still diffusion of carbon through the alloy.

At present there does not appear to be a single explanation which will account for all the differences in behavior observed between these metals when supported on silicon.

#### APPENDIX

Consider a species P diffusing through a cylindrical pellet as indicated in Fig. 7.

Let  $L$  and  $a$  be the length and radius, respectively, and assume  $a/L$  to be constant;  $l$  the mean free path for collisions of carbon atoms in the metal,  $r$  the radial distance of P from the axis and  $z$  the axial distance from Face 1.

At the outer cylindrical surfaces of the pellet we assume that carbon atoms are captured into a thin skin. If the mean free path for scattering is much less than  $a$ , then the density of carbon atoms near the sur-

faces of the cylinder will be small (due to capture). Depending on how the carbon atoms are distributed initially on Face 1, the density inside the pellet will be given by a sum of terms such as

$$\{A \exp[-\alpha_n z] + B \exp[\alpha_n z]\} J_0(\alpha_n r), \quad (1)$$

where  $\alpha_n$  are given by

$$J_0(\alpha_n a) = 0. \quad (2)$$

$J_0(\alpha_n a)$  is a Bessel function with argument  $\alpha_n a$ . The first solution of Eq. (2) gives  $\alpha_0 a = 2.4048$ .

On integrating expression (1) over  $r$  the integrating term is

$$\int_0^a 2\pi r J_n(\alpha_n r) dr, \quad (3)$$

and this varies as  $a^{-2}$ .

The current of carbon atoms per unit area through Face 2 is given by

$$-\frac{1}{3} \frac{\partial n}{\partial z},$$

where  $n$  is the carbon atom density.

Differentiating (1) with respect to  $z$  introduces a factor  $\alpha_n$ . For example,  $\alpha_0$  varies as  $a^{-1}$ .

Therefore, the number of carbon atoms per unit area leaving Face 2 in unit time varies inversely with the radius of the metal particle. Similar solutions are obtained for a truncated cone-shaped particle, which is probably a better approximation to the real condition.

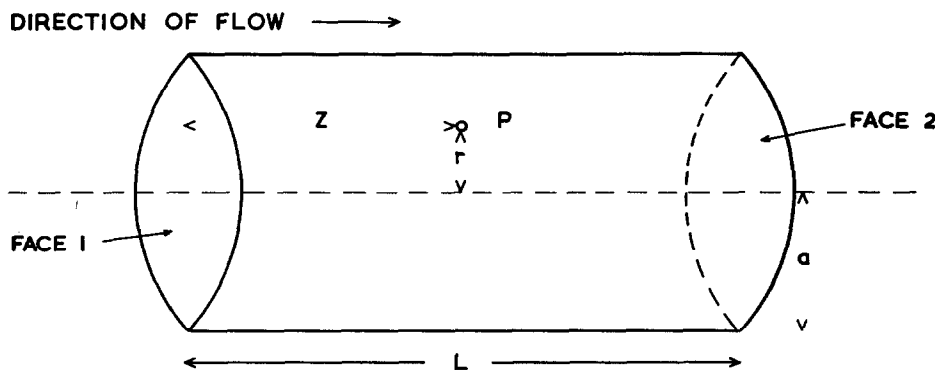


FIGURE 7

## ACKNOWLEDGMENTS

The authors are indebted to Mr. J. Wright (Applied Chemistry Division, AERE Harwell) and Dr. J. H. Tait (Theoretical Physics Division, AERE Harwell) for helpful and stimulating discussions.

## REFERENCES

1. BAKER, R. T. K., BARBER, M. A., FEATES, F. S., HARRIS, P. S., AND WAITE, R. J., *J. Catal.* **26**, 51 (1972).
2. BAKER, R. T. K., FEATES, F. S., AND HARRIS, P. S., *Carbon (Oxford)* **10**, 93 (1972).
3. ROBERTSON, S. D., *Carbon (Oxford)* **8**, 365 (1970).
4. RUSTON, W. R., WARZEE, M., HENNAUT, J., AND WATY, J., *Carbon (Oxford)* **7**, 47 (1969).
5. PRESLAND, A. E. B., AND WALKER, P. L., JR., *Carbon (Oxford)* **7**, 1 (1969).
6. LOBO, L. S., AND TRIMM, D. L., *Nature Phys. Sci.* **234**, 15 (1971).
7. PALMER, H. B., AND CULLIS, C. F., "Chemistry and Physics of Carbon" (P. L. Walker, Jr., Ed.), Vol. 1. Dekker, New York, 1965.
8. BAKER, R. T. K., AND HARRIS, P. S., *J. Phys. E: Sci. Instrum.* **5**, 793 (1972).
9. MORGAN, D. W., AND KITCHENER, J. A., *Trans. Faraday Soc.* **50**, 51 (1964). GRACE, R. E., AND DERGE, G., *Trans. AIME* **212**, 331 (1958).
10. KOVENSKIY, I. I., *Phys. Metals Metallogr. (USSR)* **16**, 107 (1963).
11. BORISOV, E. V., GRUZIN, P. L., AND ZEMSKII, S. V., *Zashch. Pokrytiya Metal.* **2**, 104 (1968).
12. DIAMOND, S., AND WERT, C., *Trans. AIME* **239**, 705 (1967). SHAVENSIN, A. B., MINKEVITCH, A. H., AND SCHERBINSKI, C. B., *Izv. Vyssh. Uchebn. Zaved. Chern. Met.* **1**, 95 (1965). GRUZIN, P. L., POLICKARPOV, Y. A., AND FEDEROV, G. B., *Phys. Metals Metallogr. (USSR)* **4**, 94 (1957).
13. BAKER, R. T. K., AND THOMAS, R. B., *J. Cryst. Growth* **12**, 185 (1972).
14. BARANIECKI, C., PINCHBECK, P. H., AND PICKERING, F. B., *Carbon (Oxford)* **7**, 213 (1969).
15. WAGNER, R. S., AND DOHERTY, C. J., *J. Electrochem. Soc.* **115**, 93 (1968).
16. BAKER, R. T. K., HARRIS, P. S., AND WAITE, R. J., unpublished results.